Nuclear Congression and Membrane Fusion:
Two Distinct Events in the Yeast Karyogamy Pathway

Laurie Jo Kurihara, Christopher T. Beh, Martin Latterich,* Randy Schekman,* and Mark D. Rose

Lewis Thomas Laboratory, Princeton University, Princeton, New Jersey 08544; and *The Howard Hughes Medical Institute and Department of Molecular and Cell Biology, University of California, Berkeley, California 94720

Abstract. Karyogamy is the process where haploid nuclei fuse to form a diploid nucleus during yeast mating. We devised a novel genetic screen that identified five new karyogamy (*KAR*) genes and three new cell fusion (*FUS*) genes. The *kar* mutants fell into two classes that represent distinct events in the yeast karyogamy pathway. Class I mutations blocked congression of the nuclei due to cytoplasmic microtu-bule defects. In Class II mutants, nuclear congression proceeded and the membranes of apposed nuclei were closely aligned but unfused. In vitro, Class II mutant membranes were defective in a homotypic ER/nuclear membrane fusion assay. We propose that Class II mutants define components of a novel membrane fusion complex which functions during vegetative growth and is recruited for karyogamy.

I N the yeast *Saccharomyces cerevisiae*, the nuclear envelope remains intact throughout mitosis, meiosis, and mating (Byers, 1981). Consequently, the yeast microtubule organizing center, the spindle pole body (SPB)[1], is embedded within the nuclear envelope and nucleates both intranuclear and cytoplasmic microtubules. The formation of a diploid nucleus during mating requires the sequential fusion of two haploid cells followed by fusion of their nuclei. Both cell fusion and nuclear fusion (karyogamy), require prior activation by mating pheromone (Rose et al., 1986). Mutations in three genes, *FUS1*, *FUS2*, and *FUS3*, cause defects in cell fusion by interfering with the breakdown of the septum between the mating cells (Trueheart et al., 1987; McCaffrey et al., 1987; Elion et al., 1990). Cytological observation of zygotes suggested that karyogamy is mediated by cytoplasmic microtubules that extend from the SPBs and interconnect the two nuclei (Byers and Goetsch, 1974, 1975). Concomitant with cytoplasmic microtubule depolymerization, nuclei appeared to be drawn together and fused along one edge of the apposed SPBs.

Genetic studies have confirmed the requirement for microtubules and the SPB during karyogamy (Rose, 1991). Analysis of *TUB2*, the yeast β-tubulin gene, and *BIK1*, which encodes a microtubule-associated protein, demonstrated that cytoplasmic microtubules are essential for karyogamy (Huffaker et al., 1988; Berlin et al., 1990). A mutation in either gene destabilizes microtubules, which prevents karyog-amy from proceeding. The kinesin-related gene, *KAR3*, is required to cross-bridge opposing microtubules and generate force for their movement (Meluh and Rose, 1990). Kar3p physically interacts with Cik1p, another protein required for karyogamy; Cik1p localizes to the SPB and microtubules and null mutations cause defects similar to *kar3* mutations (Page and Snyder, 1992; Page et al., 1994). During karyogamy, *KAR3* has also been implicated in depolymerization of cytoplasmic microtubules at the SPB, possibly through an interaction with a SPB component, *KAR1* (Rose and Fink, 1987; Vallen et al., 1992). The SPB may act at multiple stages during nuclear fusion; it is required for microtubule organization but it is unknown whether membrane fusion is also mediated by the SPB or by other proteins.

The role of *KAR2* during karyogamy has been less clear. Because *KAR2* encodes the yeast BiP/GRP78 homolog, which is localized to the lumen of the nuclear envelope and ER (Rose et al., 1989), two general models have been proposed. First, Kar2p might act indirectly in the assembly of SPB or other components required for karyogamy. In this case, *kar2* mutants would be expected to show defects similar to *kar* mutants that directly affect the function of the SPB and microtubules. Second, Kar2p may play a more direct role in the assembly or disassembly of protein complexes required for fusion of the membranes. In this case, *kar2* mutants would be expected to show defects in membrane fusion. In material to be published elsewhere (Latterich and Schekman, 1994) and in this manuscript, evidence is presented which suggests that Kar2p plays a more direct role in nuclear envelope fusion.

The original screen for karyogamy mutants identified mutations in *KAR1*, *KAR2*, and *KAR3* but not *TUB2* or other genes later found to be required for karyogamy (Conde and Fink, 1976; Polaina and Conde, 1982). This bias arises be-

---

1. *Abbreviations used in this paper*: gpαF, glycosylated pro-α-factor; SPB, spindle pole body.

cause *kar* mutations behave in two different ways during mating. Unilateral mutations display fusion defects when mated to wild type. In contrast, bilateral mutations display fusion defects only when both parents are mutant. Some unilateral mutations are dominant, e.g., *kar3-1* (Meluh and Rose, 1990). Alternatively, mutations may be unilateral because the gene products are restricted to a specific compartment, e.g., *KAR2* (Rose et al., 1989), or required for functions before cell fusion, e.g., *KAR1* (Rose and Fink, 1987). In these examples, the wild-type protein is either inactivated by the mutant protein or limited in its action to one of the two nuclei. In the latter case, it is assumed that the protein must act on both nuclei for fusion to proceed. For bilateral mutations, the gene products are presumed to be either redundant or diffusible and capable of functioning after cell fusion. Thus, a mutant phenotype is observed only when both parents are deficient. Mutations in *TUB2* and recessive *kar3* mutations cause bilateral defects (Huffaker et al., 1988; Meluh and Rose, 1990).

The original screen for karyogamy mutants required that the mutations act unilaterally and has been effectively saturated (Conde and Fink, 1976; Polaina and Conde, 1982). Isolation of bilateral *kar* mutations has been technically challenging. The bilateral mutations that are known were either found serendipitously, e.g., *BIK1* and *FUS1* (Trueheart et al., 1987; Berlin et al., 1990), or by analyzing genes predicted or known to be required for karyogamy, e.g., *TUB2* and *KAR3* (Huffaker et al., 1988; Meluh and Rose, 1990). An earlier screen to isolate bilateral mutations (Berlin et al., 1991) used the *HO* gene to generate strains in which the same mutation was present in both mating types, thereby allowing candidate mutants to be self-crossed. Although *fus3-1* was isolated from this screen, the use of *HO* made subsequent steps technically difficult and no new bilateral karyogamy mutants were identified.

In this paper we describe a novel bilateral mutant screen that uses a rapid and simple method to switch mating type so as to self-cross each mutant. Using this screen, we identified five new *KAR* genes and three new *FUS* genes. The *kar* mutants were divided into two distinct classes which define two steps along the pathway for karyogamy. Class I mutations affect the congression of the nuclei via SPB or cytoplasmic microtubule defects. This class includes *kar1*, *kar3*, *kar4*, and *kar9* mutations. Class II mutations do not affect nuclear congression but appear to be defective for nuclear membrane fusion. This novel class includes *kar2*, *kar5*, *kar7*, and *kar8* mutations. We propose that the Class II mutants define a membrane fusion apparatus that is required for nuclear fusion during mating and which performs other functions during vegetative growth.

Materials and Methods

Strains and Microbial Techniques

Yeast strains used in this study are listed in Table I. Yeast media and genetic techniques were essentially as described in Rose et al. (1990). Yeast transformations were performed according to Ito et al. (1983). Yeast DNA for Southern analysis was prepared by the method of Hoffman and Winston (1987). Southern blots and hybridizations were performed according to Rose et al. (1990). Quantitative matings were performed according to Meluh and Rose (1990). ρ^0 strains were induced using ethidium bromide as described in Rose et al. (1990). Cells were mutagenized with ethyl

methanesulfonate (Eastman Kodak) as described in Rose et al. (1990). Cells used for this study were mutagenized to 40% viability with a 100-fold increase in canavanine resistance.

Strain Construction

A *mat*Δ was generated using plasmid B940 which carries *MAT*α deleted for the *MAT*α*1* and *MAT*α*2* genes and replaced by *LEU2* (Mahoney and Broach, 1989). *ScaI* sites within *MAT*α were used to purify the fragment for transplacement at the chromosomal *MAT*α locus of MS52. Leu+ transformants were confirmed as *mat*Δ alleles by a switch from α to a mating type, a failure to sporulate when mated to a wild-type α strain, and by Southern blot analysis.

To construct the ploidy assay cassette, a 430-bp *KpnI/NdeI*-blunt fragment of *HIS3* was purified from plasmid B886 (provided by Jim Broach). It was cloned into *KpnI*, *SmaI* of pRS304, an integrating *TRP1* vector (Sikorski and Hieter, 1989). This construct was cut with *BglII* internal to the *HIS3* insert and transplaced to the *HIS3* chromosomal locus of the *mat*Δ strain generated above. Trp+ transformants were confirmed as integrants at *HIS3* by an associated His- phenotype and by Southern blot analysis. This construction generated direct repeats of *HIS3* sequence which allow the *TRP1* insert to loop out by homologous recombination. This results in the formation of papillae which arise from outgrowth of individual cells that have become His+ in a background patch of His- cells. Integrants were tested for their ability to become His+ by formation of papillae on SC-His medium. The locus was also tested for its ability to distinguish ploidy. Diploids containing the locus formed numerous papillae compared to their haploid counterparts.

The YCp50 based *MAT*α plasmid B1311 (provided by Jim Broach) was transformed into the *mat*Δ, ploidy assay strain. As predicted, Ura+ transformants mated efficiently as α and 5-FOA resistant isolates mated as a. When grown on rich medium which allowed plasmid loss and mating, numerous papillae formed on SC-His-Trp medium compared to patches grown under maintained selection for the plasmid. To determine whether the papillation assay would distinguish between Kar+ and Kar- phenotypes, a *kar1*Δ*15* allele was transplaced into MS2104. A YIp5 plasmid containing the *kar1*Δ*15* allele (pMR1593) was cut with *BglII* and integrated at the chromosomal *KAR1* locus. Ura- loop outs were selected on 5-FOA medium and subsequently tested for a Kar- phenotype.

For in vitro homotypic membrane fusion assays, the *pep4*Δ::*URA3* and *gls1-1* (Esmon et al., 1984) mutations were crossed into the *kar* mutant strains. Segregation of the *gls1-1* mutation was assayed by Western blot for mobility shifts in modification of the Eug1 protein (Tachibana and Stevens, 1992).

Complementation Analysis

Mating diploids were constructed for complementation tests. The a form of each mutant was maintained as Trp+, His- and the α form was maintained as Trp-, His+. Matings in all combinations were performed and heterozygous double mutant diploids were selected on SD min. The diploids were capable of mating due to the *mat*Δ allele. Because the mutations were bilateral, each mating diploid was then mated to the corresponding haploid a and α mutants. For example, a *karX/karY* mating diploid was mated to both *karX* and *karY* haploids and tested for complementation of both mutations by plate mating assays or microscopy. In addition to using mating diploids, complementation analysis was also performed by mating haploid bilateral mutations in all combinations. The same results were obtained using both assays.

For complementation tests against known genes, *kar3::LEU2* (Meluh and Rose, 1990) and *bik1-518* (Berlin et al., 1990) mutations were used to construct mating diploids. For other known genes, wild-type plasmids were transformed and tested for suppression of Kar- or Fus- defects. These include *TUB2*, *CIK1*, *FUS1*, *FUS2*, and *FUS3*.

Nuclear Distance Measurements

Microscopy assays were performed as described in Rose et al. (1990). Approximately 5×10^6 exponentially growing cells of each parent were mixed together and concentrated on a 0.45-μm pore size nitrocellulose filter. The mating mixtures were incubated for 2 h on YEPD at 30°C and fixed in methanol/acetic acid (3:1) at 4°C for several hours. Zygotes were washed with PBS and resuspended in PBS containing the fluorescent, DNA specific dye DAPI (4',6'-diamidino-2-phenylindole) at 1 μg/ml. Zygotes were then analyzed by DIC and UV for DAPI on a Zeiss axiophot micro-

Table I. Yeast Strains Used in This Study

Strain	α Strain*	Genotype	Source
MS2073	MS2104	*matΔ::LEU2 ura3-52 leu2-3,112 trp1Δ1 his3::TRP1*	This Study
	MS2101	MS2073 *kar1-Δ15*	This Study
MS2710	MS2709	MS2073 *kar4-2150*	This Study
MS2690	MS2689	MS2073 *kar5-486*	This Study
MS2686	MS2685	MS2073 *kar5-1162*	This Study
MS2682	MS2681	MS2073 *kar7-1039*	This Study
MS2706	MS2705	MS2073 *kar8-1333*	This Study
MS2684	MS2683	MS2073 *kar9-485*	This Study
MS2328	MS2326	MS2073 *fus5-424*	This Study
MS2742	MS2741	MS2073 *fus5-1325*	This Study
MS2744	MS2743	MS2073 *fus5-1829*	This Study
MS2680	MS2679	MS2073 *fus6-964*	This Study
MS2748	MS2747	MS2073 *fus6-2092*	This Study
MS2746	MS2745	MS2073 *fus7-1811*	This Study
MS2750	MS2749	MS2073 *fus2-410*	This Study
MS1268		*MATα leu2-3,112 ade2-101 kar1-1*	Vallen et al., 1992
MS1269		*MATa ade2-101 trp1Δ1 lys2-801 kar1-1*	Vallen et al., 1992
MS1273		*MATα leu2-3,112 ade2-101 trp1Δ1 kar1-Δ13*	Vallen et al., 1992
MS1274		*MATa ura3-52 trp1Δ1 lys2-801 kar1-Δ13*	Vallen et al., 1992
MS1271		*MATα leu2-3,112 ura3-52 trp1Δ1 kar1-Δ15*	Vallen et al., 1992
MS1272		*MATa ura3-52 trp1Δ1 lys2-801 kar1-Δ15*	Vallen et al., 1992
MS1000		*MATα ura3-52 trp1Δ1 kar2-1*	Rose et al., 1989
MS1111		*MATa ura3-52 leu2-3,112 ade2-101 kar2-1*	Rose et al., 1989
MS177		*MATα ura3-52 ade2-101 kar2-159*	Rose et al., 1989
MS175		*MATa ura3-52 leu2-3,112 trp1Δ1 kar2-159*	Rose et al., 1989
MS1715		*MATα leu2-3,112 ade2-101 kar2-133*	This Study
MS1714		*MATa leu2-3,112 ade2-101 kar2-133*	This Study
MS531		*MATα ura3-52 leu2-3,112 trp1Δ1 kar3Δ::LEU2*	Meluh and Rose, 1990
MS524		*MATa ura3-52 leu2-3,112 ade2-101 kar3Δ::LEU2*	Meluh and Rose, 1990
MS3212		*MATα ura3-52 leu2-3,112 his3Δ200 ade2-101 kar4Δ::HIS3*	This Study
MS3216		*MATa ura3-52 leu2-3,112 his3Δ200 ade2-101 kar4Δ::HIS3*	This Study
MS3181		*MATα ura3-52 ade2-101 his3Δ200 kar1-Δ15 kar2-159*	This Study
MS1306		*MATa ura3-52 leu2-3,112 kar1-Δ15 kar3Δ::LEU2*	This Study
MS3185		*MATα ura3-52 his3Δ200 kar1-Δ15 kar4Δ::HIS3*	This Study
MS3252		*MATa ura3-52 kar1-Δ15 kar5-486*	This Study
MS3254		*MATa ura3-52 kar1-Δ15 kar5-1162*	This Study
MS3255		*MATa ura3-52 trp1Δ1 kar1-Δ15 kar7-1039*	This Study
MS3256		*MATa ura3-52 trp1Δ1 kar1-Δ15 kar8-1333*	This Study
MS3179		*MATα ura3-52 leu2-3,112 his3Δ200 kar2-159 kar3Δ::LEU2*	This Study
MS3187		*MATα ura3-52 leu2-3,112 his3Δ200 kar2-159 kar4Δ::HIS3*	This Study
MS3183		*MATα ura3-52 leu2-3,112 his3Δ200 kar3Δ::LEU2 kar4Δ::HIS3*	This Study
MS3184		*MATa ura3-52 leu2-3,112 his3Δ200 kar3Δ::LEU2 kar4Δ::HIS3*	This Study
L2751		*MATα ura3-52 leu2-3,112 bik1-518*	Berlin et al., 1990
MLY1601		*MATa ura3-52 leu2-3,112 pep4Δ::URA3 gls1-1*	Latterich and Schekman, 1994
MY3257		*matΔ ura3-52 leu2-3,112 pep4::URA3 kar5-486*	This Study
MY3258		*MATa ura3-52 leu2-3,112 pep4::URA3 kar5-486 gls1-1*	This Study
MY3259		*MATa ura3-52 leu2-3,112 pep4::URA3 kar5-1162*	This Study
MY3260		*matΔ ura3-52 leu2-3,112 pep4::URA3 kar5-1162 gls1-1*	This Study
MY3254		*MATa ura3-52 leu2-3,112 pep4::URA3 kar7-1039*	This Study
MY3253		*MATa ura3-52 leu2-3,112 pep4::URA3 kar7-1039 gls1-1*	This Study
MY3256		*MATa ura3-52 leu2-3,112 pep4::URA3 kar8-1333*	This Study
MY3255		*MATa ura3-52 leu2-3,112 pep4::URA3 kar8-1333 gls1-1*	This Study

α strains* are isogenic to *matΔ::LEU2* forms except for the presence of [*YCpMATα*].

scope. Nuclear distance was measured using a SIT camera and processed using an image analysis program, OMNEX (Imagen, Princeton, NJ).

Two measurements were taken for each zygote: the inner edge to edge distance between the two nuclei and the outer edge to edge distance which also included the nuclear diameters. A third value was calculated by averaging the first two measurements which corresponds to the nuclear center to center distance. This value controlled for slight variability in the intensity of the DAPI staining. Means and standard deviations were calculated from measurements of 35 zygotes. When performing these assays, only unbudded

zygotes were examined. Once a bud emerged, both nuclei migrated toward the bud neck for mitosis, regardless of the mutant class. This suggests that nuclear migration for karyogamy and mitosis are differentially controlled within the zygote.

Microscopy

Indirect immunofluorescent staining of yeast cells was performed as described in Rose and Fink (1987). Zygotes were prepared as above for tubulin

and Kar2p staining. Rabbit Antiserum (RAP124) directed against yeast β-tubulin was provided by Frank Solomon. Kar2p antiserum was used as described in Rose et al. (1989). Fluorescein isothiocyanate-conjugated secondary antibodies were purchased from Boehringer Mannheim Biochemicals (Indianapolis, IN). Permanganate fixation for electron microscopy was performed according to Kaiser and Schekman (1990) with the following modification: cells were treated with glutaraldehyde for 45 min at room temperature. Sections were cut to 70 nm, stained with lead citrate, and examined in a Jeol 100C TEM at 80 kV. A crude estimate of the total number of membrane bridges which may be present between apposed nuclei was based upon an estimate of the maximum diameter of the zone of apposition (about 1 mm), the thickness of the sections (about 70 nm) and the observed frequency of bridges in random sections (12 out of 30 sections) through the zone of apposition. These numbers predict an average of 5 to 6 bridges between each pair of nuclei. Given these assumptions it is unlikely that our estimate is in error by more than a factor of 2.

In Vitro Assay for Homotypic Membrane Fusion

Strains were constructed as described above. Membrane isolation and fusion assays were performed as described by Latterich and Schekman (1994). In all cases, strains were grown and membranes prepared at 30°C. 75 μg glsl-1 membranes containing untrimmed gpαF were mixed with 75 μg of wild-type yeast microsomes, and an ATP regeneration system, in a total volume of 50 μl. Fusion was allowed for 1 h at either 30°C or 37°C, as indicated. Chilled reactions were treated with trypsin, and then trypsin inhibitor to degrade gpαF that was not membrane enclosed. Reactions were terminated by the addition of 60 μl of 2× Laemmli sample buffer with 2% β-ME and resolved in a 12.5% SDS-PAGE. Gels were fixed, dried, and exposed to phosphor plates. The percentage of glucose trimming (i.e., the conversion of the 32-kD glsl-1 form of gpαF to the 29-kD wild-type form) was quantified using standard software in a Phosphorimager (Molecular Dynamics, Sunnyvale, CA).

Results

Identification of New KAR and FUS Genes

The screen for bilateral mutants is comprised of three parts. First, each mutant is generated in both mating types and self-crossed. Second, a papillation assay is used to detect mating defects. Finally, microscopy identifies the kar and fus mutants among the candidate mutants.

The first step, a rapid-mating type switch (Fig. 1 A), is based upon the observation that a matΔ strain mates as an a (Kassir and Simchen, 1976). Because the deletion is recessive, a matΔ strain mates as an α when a MATα plasmid is present. Therefore plasmid loss effectively switches mating type from α to a. When grown under selection for the MATα plasmid, cells in a colony are primarily α haploids. Without selection, the plasmid is lost at a few percent per generation (Koshland and Hieter, 1987). Having lost the plasmid, the resulting a cells are in proximity to mate with α cells that have retained the plasmid. Thus a wild-type colony becomes a mixture of a and α haploids and accumulates diploids. A mating defective colony remains a mixture of a and α haploids only.

In the second step, we used an assay for ploidy to determine whether mating had occurred. Since both mating parents had precisely the same genotype, diploids could not be distinguished from haploids by auxotrophic markers. The method of Chan and Botstein (1993) was used to indirectly measure diploid formation (Fig. 1 B). The TRP1 gene was integrated to disrupt the chromosomal HIS3 gene; this confers a Trp+, His− phenotype. Direct repeats of HIS3 sequence flanking TRP1 allow the disruption to revert by homologous recombination, thereby restoring a Trp−, His+ phenotype. Haploids possess only one chromosomal copy of
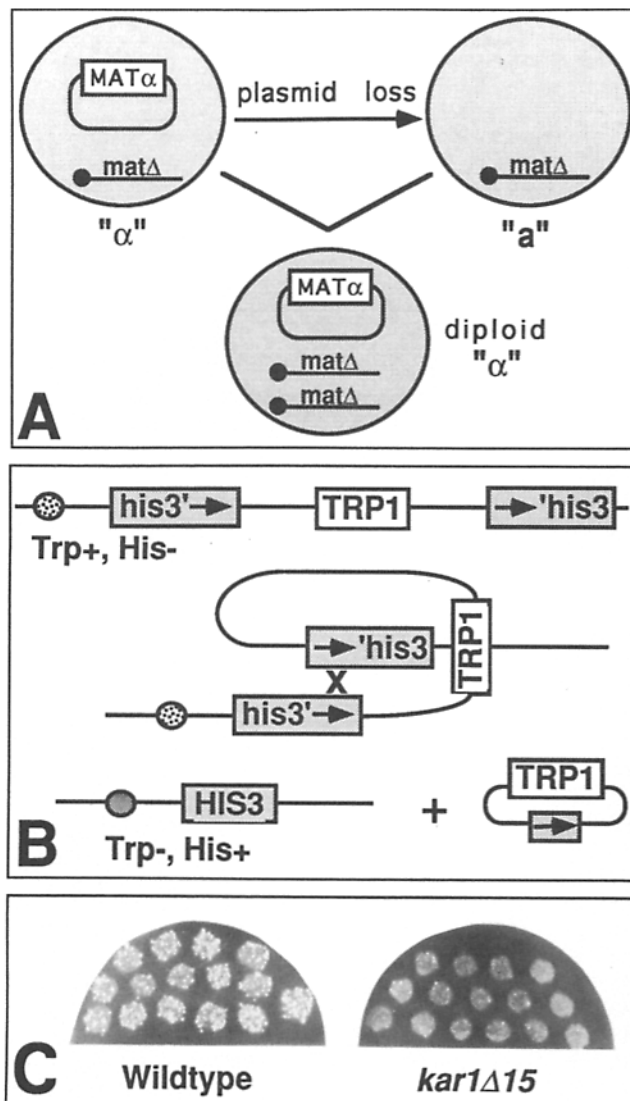
Figure 1. Schematic of the bilateral mutant screen. (A) A rapid method to switch mating type. A matΔ strain mates as an a. When a MATα plasmid is present, the matΔ strain mates as an α. Plasmid loss effectively switches mating type. Colonies grown under nonselective conditions for the plasmid contain a mixture of a and α cells which then mate to produce diploids. (B) A papillation assay to distinguish ploidy. The TRP1 gene was integrated at HIS3, conferring a Trp+, His− phenotype; TRP1 can loop out to produce a Trp−, His+ phenotype. Haploids possess one copy and are either His+ or Trp+, but not both. Diploids possess two copies of this locus and can become both His+ and Trp+. (C) Karyogamy mutants display a reduced papillation phenotype. Wild-type (MS2104) colonies form many diploids which then produce many papillae on medium lacking histidine and tryptophan. The karyogamy defective mutation kar1Δ15 (MS2101) forms few diploids and thus few papillae.

the locus and are either Trp+ or His+, but not both, depending on whether TRP1 is integrated or has reverted. Because diploids possess two copies of the locus they can become both Trp+ and His+ when only one of the disrupted HIS3 loci reverts. Therefore, wild-type diploids produce numerous His+, Trp+ papillae on medium lacking histidine and tryptophan whereas haploids produce few in any. In conse-

quence, the wild-type parent produces many papillae due to efficient diploid formation whereas mutants defective for diploid formation form very few papillae, e.g., *kar1Δ15* (Fig. 1 *C*).

Out of 40,000 mutagenized colonies, 665 showed reduced papillation after several rounds of rescreening. In addition to mutations that affect mating, reduced papillation could be the result of several other defects. Mutations in any gene required for histidine or tryptophan biosynthesis would prevent growth on medium lacking these nutrients. Similarly, a mutant defective for homologous recombination would be unable to revert to His⁺. 14 *trp* mutants and 88 presumed *rec* or *his* mutants were eliminated leaving 563 putative mating defective mutants.

The final step of the screen entailed microscopic examination of zygote morphology to identify *kar* and *fus* mutants among the remaining non-papillators. First, it was necessary to generate stable forms of both mating types of each candidate mutant. The **a** mating strains resulting from plasmid loss were selected on 5-FOA medium (Boeke et al., 1984) while the α mating strains were maintained on selective medium for the plasmid. At this step, 62 mutants displayed unusually lush growth on 5-FOA in comparison to wild type. All proved to be sterile mutants which are more capable of growth after segregation of the *MATα* plasmid. First, after plasmid loss, sterile mutants do not mate with their plasmid bearing neighbors which would cause them to regain the plasmid and remain 5-FOA sensitive. Second, the growth of certain **a**-specific steriles, e.g., *STE2*, is not inhibited by α-factor which is secreted by their plasmid bearing neighbors. Because they fail to respond to pheromone, they do not arrest in G1. These observations might be useful in future screens for sterile mutants. The sterile mutants were eliminated at this step to further reduce the number of candidate mutants to be assayed by microscopy.

Another class of mutants potentially identified by this screen are bilateral steriles, mutants that fail to form zygotes when self-crossed. Their existence has not been demonstrated because only unilateral screens for sterile mutants have been performed. A bilateral sterile could represent any gene product that is redundant, such that only one parent would require its function for efficient zygote formation. During microscopic examination of the candidate mutants, 20 were found that failed to form zygotes when self-crossed but which mated efficiently to wild type when assayed by plate mating. Their characterization may define a novel class of sterile mutants.

After generating each candidate mutant in stable forms of both mating types, the remaining 501 candidates were examined. Zygotes were harvested from matings performed for each mutant and stained with DAPI to determine their nuclear morphology. Representative zygotes are depicted in Fig. 2. A wild-type zygote possessed a single nucleus (Fig. 2, *A* and *B*). In a *fus* mutant zygote, the nuclei remained separated by a prominent septum indicative of a block in cell fusion (Fig. 2, *C* and *D*). Fig. 2, *E–I* show three representative mutant zygotes in which cell fusion but not karyogamy has proceeded. By microscopy, 12 candidate *kar* mutants, 12 candidate *fus* mutants, and the 20 additional steriles mentioned above were identified; the remainder appeared to be wild type. To determine whether the mutants were tractable genetically, tetrad analysis was performed for each mutant
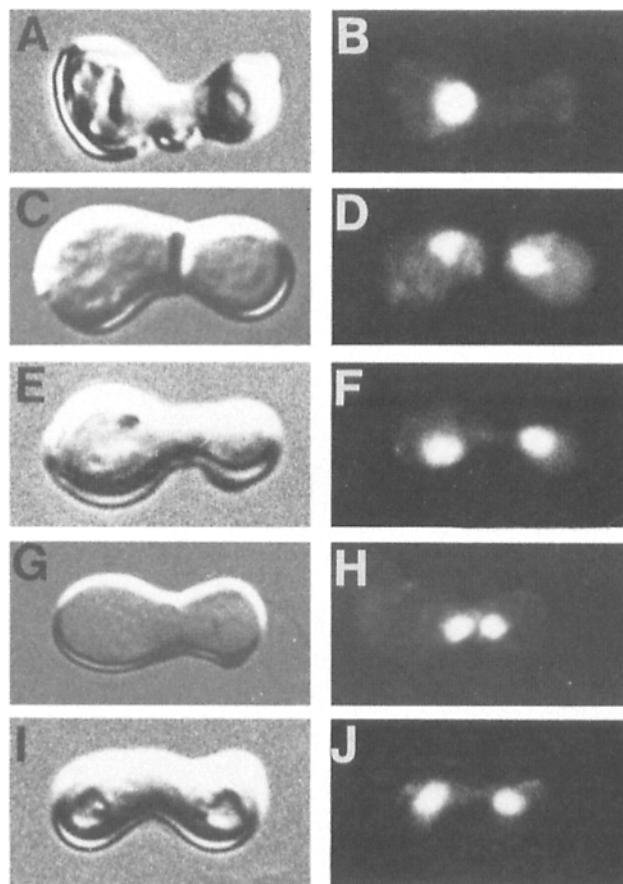
Figure 2. Two classes of *kar* mutants. Representative zygotes are presented for each category described below. (*A* and *B*) A wild-type zygote has a single fused nucleus (MS10 × MS52). (*C* and *D*) A *fus* mutant zygote has a septum present where the cells attempt to fuse (MS2749 × MS2750). (*E* and *F*) A Class I *kar* mutant zygote has two nuclei that remain far apart (MS2709 × MS2710). (*G* and *H*) A Class II *kar* mutant zygote has two nuclei that are juxtaposed (MS2689 × MS2690). (*I* and *J*) A Class I/Class II double mutant zygote displays a Class I phenotype (MS3181 × MS10). Zygotes were visualized by DIC (*A, C, E, G,* and *I*) and by DAPI staining for nuclei (*B, D, F, H,* and *J*).

following a back-cross to wild type. 6 *kar* mutants and 7 *fus* mutants showed 2:2 segregation, indicating that the phenotypes resulted from single nuclear mutations.

To determine the number of genes affected, it was necessary to test dominance and to conduct complementation tests. To test *kar* and *fus* mutants, it was necessary to construct diploids that remained capable of mating. The *matΔ* strain background facilitated the construction of the mating diploids; *MATα/matΔ* diploids mate as α and *matΔ/matΔ* diploids mate as **a**. The disrupted *HIS3* locus generated selectable markers for construction of all possible double mutant diploid combinations; the **a** strains were maintained as Trp⁺, His⁻ and the α strains were maintained as Trp⁻, His⁺. Using this approach, all heterozygous mating diploids constructed between wild type and mutant displayed essentially wild-type mating phenotypes when back-crossed to the original mutant. This demonstrated that the mutations were recessive. For complementation tests, all *kar* and *fus* mutants were crossed against one another to generate mating

A

	kar9-485	kar8-1333	kar7-1039	kar5-1162	kar5-486	kar4-2150
kar4-2150	+	+	+	+	+	−
kar5-486	+	+	+	−	−	
kar5-1162	+	+	▧	−		
kar7-1039	+	+	−			
kar8-1333	+	−				
Kar9-485	−					

					−	fus2-410
				−	+	fus7-1811
			−	+	+	fus6-2092
		−	−	+	+	fus6-964
	−	+	+	+	+	fus5-1325
−	−	+	+	+	+	fus5-1829
−	−	−	+	+	+	+	fus5-424

fus5-424, fus5-1829, fus5-1325, fus6-964, fus6-2092, fus7-1811, fus2-410 — **B**

Figure 3. Complementation analysis. (*A*) *KAR* complementation analysis. The six *kar* mutations fell into five complementation groups. *KAR4*, *KAR7*, *KAR8*, and *KAR9* had single alleles and *KAR5* had two alleles. *kar5-1162* failed to complement both *kar5-486* and *kar7-1039*. Linkage studies determined that 486 and 1162 were allelic (*KAR5*) and that 1039 was unlinked (*KAR7*). Grey boxes denote allelism; the hatched box denotes unlinked noncomplementation. (*B*) *FUS* complementation analysis. The seven *fus* mutations fell into four separate complementation groups. *FUS5* contained three alleles (424, 1829, and 1325), *FUS6* contained two alleles (964 and 2092), and *FUS7* had a single allele (1811). Mutant 410 may be a new *FUS2* allele.

diploids. Each diploid was then assayed for complementation of mating defects when back-crossed to the original mutant parents. A second approach was also used to test complementation where haploid mutants were mated in all combinations and assayed for complementation of mating defects. The same results were obtained by both methods of testing complementation.

The six *kar* mutants fell into five groups: *KAR5* contained two alleles and single alleles were obtained for *KAR4*, *KAR7*, *KAR8*, and *KAR9* (Fig. 3 *A*). The two *kar5* alleles were tightly linked but were unlinked to the *kar7* mutation (data not shown). Interestingly, *kar5-1162* did not complement the *kar7* mutation. This genetic interaction observed between *kar5-1162* and *kar7* is termed unlinked noncomplementation (Stearns and Bostein, 1988). The allele specificity of the interaction suggests that the two gene products may interact. Both *kar5-1162* and *kar7-1333* were also temperature sensitive for growth at 37°C, which suggests they may be required for functions during vegetative growth in addition to karyogamy. The seven *fus* mutants fell into four groups (Fig. 3 *B*): *FUS5* contained three alleles, *FUS6* contained two alleles, and single alleles were found for *FUS7* and mutant 410, a putative *FUS2* allele (see below).

We next determined whether the complementation groups represented new or known genes. Expected genes that would generate bilateral *kar* mutations include *KAR3*, *BIK1*, *CIK1*, and *TUB2*. Known genes that generate *fus* mutations include *FUS1*, *FUS2*, and *FUS3*. For some genes, complementation was tested by constructing heterozygous mating diploids as described above. For others, wild-type plasmids were trans-

formed into the mutants and tested for suppression of their mating defects. Using these approaches, the mutants did not fall into any of the expected complementation groups and thus represent new genes with one exception; *fus* mutant 410 was suppressed by a *FUS2* plasmid and may represent a new allele of this gene. Therefore, five new *KAR* genes and at least three new *FUS* genes have been identified.

Quantitative assays for bilateral mating defects are shown in Table II. The percentage of aberrant zygote formation was determined for each mutant by microscopy. They ranged from 40–95% when self-crossed (Table II *A*), indicating that the screen is sensitive to detect a wide range of defects. Although microscopy determines the nature (Kar⁻ or Fus⁻) of a mutant, it is a poor measurement of mating efficiency. Phenotypically mutant zygotes may eventually convert to wild-type or zygotes that appear normal may be incapable of generating diploid progeny. Therefore, quantitative matings were performed and in all cases these results were in agreement with the microscopy data. As shown in Table II *C*, all *kar* and *fus* mutants displayed a dramatic reduction in diploid formation when self-crossed. Cytoductants are progeny unique to Kar⁻ zygotes that inherit a haploid nucleus from one parent and a cytoplasmic (mitochondrial) marker from the other parent; they are a sensitive measure of karyogamy defects. The six *kar* mutants displayed dramatic increases in cytoductant formation when self-crossed (Table II *E*). Many of the mutants also exhibited very weak mating defects when crossed to wild type (Table II *B*, *D*, and *F*). However, the majority of the mutants are still considered bilateral; truly unilateral mutations display comparable defects regardless of their mating partner.

Two Classes of kar Mutants Define a Pathway for Karyogamy

While scoring the *kar* mutant zygotes by microscopy, we observed that the mutants fell into two distinct classes based upon nuclear morphology. In a Class I zygote, the nuclei remained far apart (Fig. 2, *E* and *F*). In contrast, the nuclei were closely juxtaposed in a Class II zygote (Fig. 2, *G* and *H*). This was quantitated by measurements of the distance between the two nuclei (Table III). In Class I mutants, the nuclei were between 2.3 and 3.6 μm apart, measured from the inner edges. In Class II mutants, the nuclei were less than 0.5 μm apart. Remarkably, the mutants fell discretely into these two classes; no intermediate values were observed and little variation occurred within each class. When multiple mutant alleles of the same gene were available, the same nuclear distance values were obtained. Therefore, we infer that these two classes define discrete steps in the karyogamy pathway.

To further define the classes as intermediates during karyogamy, epistasis analysis was performed. A priori, it is expected that nuclear congression would precede nuclear fusion. This predicts that a ClassI/ClassII double mutant would display a Class I phenotype. However, in wild-type zygotes nuclei start out closely juxtaposed and it is possible that a failure in fusion would result in a later separation of the nuclei. In this case the double mutant would display a Class II phenotype. Therefore, double mutants were constructed with representative Class I and Class II mutants. In all cases a Class I mutant phenotype was observed for the double mutants (Fig. 2, *I* and *J* and Table III). This indicates

Table II. Quantitative Mating Experiments

	% Mutant zygotes		% Diploid formation			C/D ratio	
	× self	× wild type	× self	× wild type		× self	× wild type
	A	B	C	D		E	F
kar4-2150	90	<5	0.4	41		62	0.09
kar5-486	90	10	0.1	51		96	0.004
kar5-1162	80	20	0.2	8		65	0.2
kar7-1039	70	<5	7	40		5	0.01
kar8-1333	80	<5	0.2	44		71	0.005
kar9-485	40	10	9	25		2.9	0.15
fus5-424	90	10	0.2	17			
fus5-1829	70	10	1.8	21			
fus5-1325	80	10	0.4	22			
fus6-964	70	20	0.2	18			
fus6-2092	90	10	0.2	14			
fus7-1811	90	20	1	19			
fus2-410	>90	30	0.1	10			
Wild type		<5		55			0.001

Mating frequencies were quantitated for each mutant when self-crossed (A, C, and E) and when crossed to wild type (B, D, and F). Columns A and B report the percent zygotes with mutant morphology as assayed by microscopy. For each mutant, results of several assays were averaged and rounded to the nearest significant digit (n > 100 zygotes). Columns C and D report the percent of diploids measured by prototroph selection/total viable cells after limited matings. Columns E and F report the ratio of cytoductants/total diploids after limited matings.

that KAR1, KAR3, and KAR4 dependent functions precede that of KAR2 and that KAR1 function precedes those of KAR5, KAR7, and KAR8. The simplest conclusion based on these results is that karyogamy is comprised of at least two distinct events and that nuclear congression precedes nuclear fusion.

Classification of the new kar mutants provides an early assessment of their functional roles during karyogamy. The

Table III. Quantitation of Distance between Zygotic Nuclei

		Distance between zygotic nuclei (μm)	
		edge to edge*	center to center‡
Class I	kar1-1	2.3 (± 0.6)	3.4 (± 0.7)
	kar1Δ13	2.7 (± 0.7)	3.7 (± 0.8)
	kar1Δ15	2.7 (± 0.6)	3.7 (± 0.7)
	kar3Δ101	3.6 (± 1.0)	4.2 (± 1.0)
	kar4-2150	2.5 (± 0.7)	3.6 (± 0.7)
	kar4Δ100	2.4 (± 0.8)	3.6 (± 0.9)
	kar9-485	2.9 (± 1.0)	3.7 (± 1.0)
Class II	kar2-1	0.3 (± 0.2)	1.7 (± 0.3)
	kar2-159	0.5 (± 0.3)	1.8 (± 0.4)
	kar2-133	0.4 (± 0.2)	1.8 (± 0.4)
	kar5-486	0.4 (± 0.2)	1.6 (± 0.3)
	kar5-1162	0.4 (± 0.3)	1.6 (± 0.3)
	kar7-1039	0.3 (± 0.2)	1.7 (± 0.3)
	kar8-1333	0.3 (± 0.2)	1.6 (± 0.2)
Class I/II	kar1Δ15/kar2-159	2.7 (± 0.8)	3.7 (± 0.9)
	kar3Δ101/kar2-159	3.2 (± 0.7)	4.4 (± 0.8)
	kar4Δ100/kar2-159	2.9 (± 0.6)	4.0 (± 0.7)
	kar1Δ15/kar5-486	2.7 (± 0.7)	3.9 (± 0.8)
	kar1Δ15/kar5-1162	2.6 (± 0.7)	3.8 (± 0.8)
	kar1Δ15/kar7-1039	2.7 (± 0.6)	4.0 (± 0.7)
	kar1Δ15/kar8-1333	2.5 (± 0.5)	3.8 (± 0.7)
Class I/I	kar1Δ15/kar3Δ101	3.4 (± 0.8)	4.7 (± 0.9)
	kar1Δ15/kar4Δ100	3.2 (± 0.7)	4.4 (± 0.8)
	kar3Δ101/kar4Δ100	3.0 (± 0.8)	4.3 (± 0.8)

Distance values were measured in μm.
* Edge to edge denotes the distance between two nuclei using their inner edges as reference (n = 35 zygotes).
‡ Center to center denotes the distance between two nuclei using the center of each nucleus as reference (n = 35 zygotes). Center to center values were obtained by averaging two measurements: the inner edge to edge measurement and the outer edge to edge measurement. This controls for size differences of nuclei caused by variability in DAPI staining.

Class I phenotype results from a defect in nuclear congression and this implies defects in microtubule or SPB functions. A Class II phenotype apparently results from defects in nuclear membrane fusion and this might imply nuclear envelope or ER defects. By these criteria, the previously characterized genes *KAR1*, *KAR2*, and *KAR3* fell into the predicted classes. It is expected that new Class I mutants *kar4* and *kar9* would exhibit microtubule-related defects and that Class II mutants *kar2*, *kar5*, *kar7*, and *kar8* would exhibit nuclear membrane fusion defects.

New Class I Mutations Cause Microtubule-related Defects

The nuclear congression defects of *kar4* and *kar9* were characterized by examining microtubule morphology in zygotes. In *kar4* mutant zygotes, abnormally long cytoplasmic microtubules were present but failed to interconnect the nuclei (Fig. 4 *B*). This phenotype was not the result of a prior defect in spindle misorientation, because in *kar4* shmoos, cytoplasmic microtubules were still directed to the shmoo tip (data not shown). These phenotypes were identical to those caused by null mutations in the kinesin-related gene, *KAR3* (Meluh and Rose, 1990), and in *CIK1* (Page and Snyder, 1992). This predicts that Kar4p may act in concert with Kar3p and Cik1p, two proteins which have been shown to physically interact (Page et al., 1994). Surprisingly, preliminary evidence indicates that Kar4p is required for pheromone induced transcription of both *KAR3* and *CIK1* but not other pheromone inducible genes (Kurihara, L. J., and M. D. Rose, manuscript in preparation).

The microtubule morphology for *kar9* mutant zygotes was unlike previously identified *kar* mutants (Fig. 4 *E*). In *kar9*, cytoplasmic microtubules were present but shorter than in *kar4*. Unlike the *kar4* mutant, the *kar9* cytoplasmic microtubules were misoriented with respect to one other. This phenotype suggests that nuclear congression failed due to defects in spindle orientation which is regulated in part by the cytoplasmic microtubules (Huffaker et al., 1988; Jacobs et al., 1988). In support of microtubule related defects, the *kar9* mutant was hypersensitive to the anti-microtubule drug, benomyl (data not shown). This suggests that in addition to karyogamy, *KAR9* may be important for vegetative cytoplasmic microtubule functions such as spindle orientation and nuclear migration during mitosis.

Class II Mutations Cause Membrane Fusion Defects

Measurement of the distance between nuclei stained with DAPI indicated that in Class II mutant zygotes, the chromatin of the two nuclei were closely juxtaposed but separate. To determine whether this morphology corresponded to a defect in nuclear envelope fusion or to a later step involving the fusion and mixing of the two genomes, the nuclear envelope of the mutants was examined by several methods.

First we used indirect immunofluorescence with antibodies against the ER/nuclear envelope lumenal marker, Kar2p (Fig. 5). As expected, in Class I mutant zygotes the nuclei were separate and surrounded by distinct nuclear envelope staining (Fig. 5 *B*). In contrast, the nuclei in Class II mutant zygotes were in close proximity, and in each case, a distinct membrane containing Kar2p separated the nuclei (Fig. 5 *E*). The Kar2p staining between the nuclei was observed in all
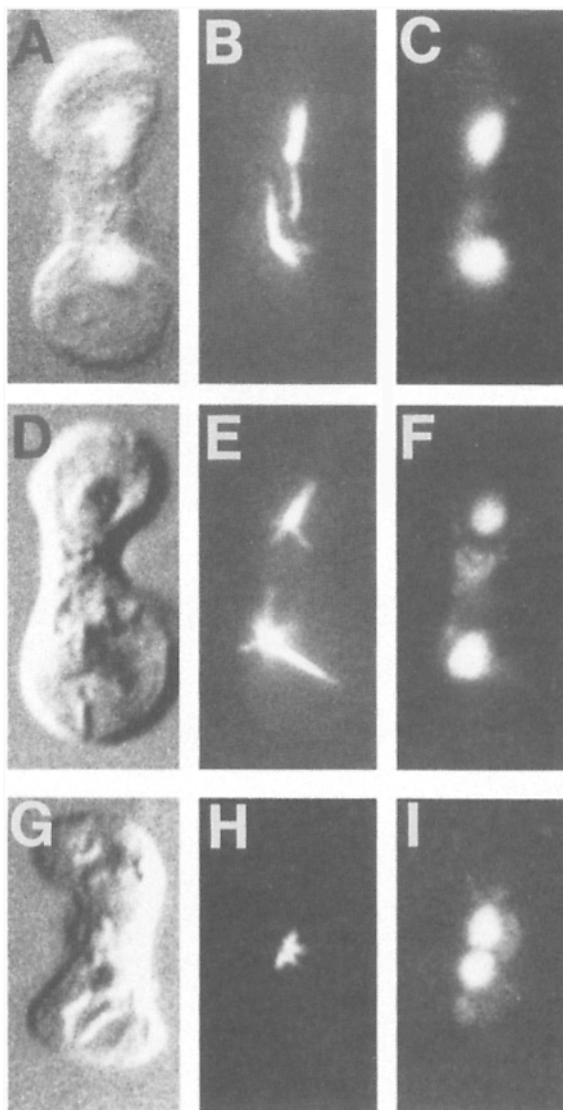
Figure 4. New Class I mutations cause microtubule defects. (*A*, *B*, and *C*) A *kar4* mutant zygote displayed cytoplasmic microtubules that were abnormally long and failed to interconnect (MS2709 × MS2710). (*D*, *E*, and *F*) A *kar9* mutant zygote displayed cytoplasmic microtubules that were present but misoriented (MS2683 × MS2684). (*G*, *H*, and *I*) A representative Class II mutant zygote displayed a normal microtubule morphology after nuclear congression (MS2689 × MS2690). All zygotes assayed (*n* = at least 25) for each mutant were uniform in morphology. Panels show zygotes by DIC (*A*, *D*, and *G*), corresponding nuclei by DAPI (*C*, *F*, and *I*), and microtubules by indirect immunofluorescence against β-tubulin (*B*, *E*, and *H*).

focal planes containing nuclei when examined by confocal microscopy (data not shown). These data suggest that the nuclear membranes were intact between the juxtaposed nuclei and that the two genomes remained in separate compartments. However, this assay cannot distinguish whether the nuclear membranes were completely unfused or in an intermediate state where, for example, the outer but not inner membranes have fused. Defects in membrane docking or recognition might result in completely unfused membranes whereas defects in the process of membrane fusion might re-
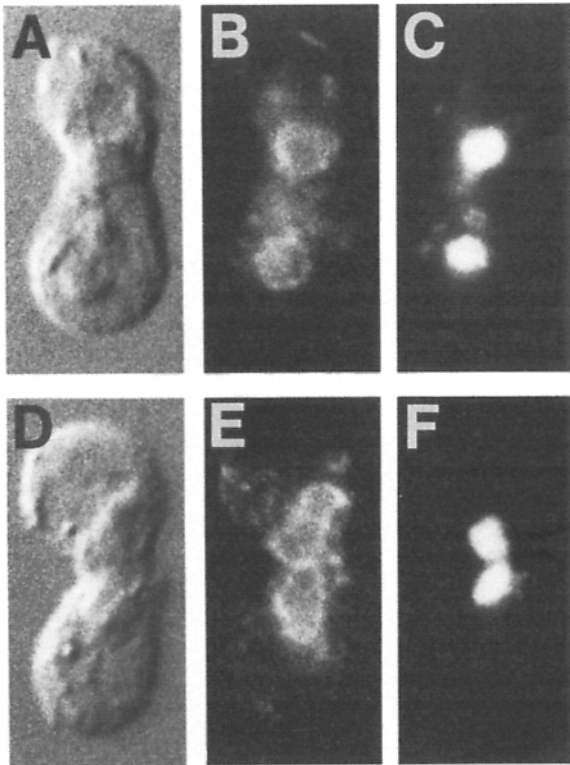
Figure 5. The membranes of Class II zygotic nuclei are juxtaposed. (*A, B,* and *C*) The nuclear membranes of Class I zygotic nuclei remain separate and distinct (MS2709 × MS2710). (*D, E,* and *F*) In a representative Class II zygote, the nuclear membranes were closely juxtaposed, but we were unable to determine by this assay if the membranes had fused (MS2689 × MS2690). All zygotes assayed (*n* = at least 25) for each Class I and Class II mutant displayed these morphologies. Panels show zygotes by DIC (*A* and *D*), corresponding nuclei by DAPI staining (*C* and *F*), and the nuclear envelope by indirect immunofluorescence against Kar2p (*B* and *E*).

sult in novel intermediates. In the latter case, nuclear envelope lumenal contents may become mixed.

To distinguish these possibilities, the nuclear membranes of Class II mutant zygotes were examined by electron microscopy. In these experiments, permanganate staining was used to emphasize membranous structures; proteinaceous nuclear pores and SPBs were not visible using this technique. As shown in Fig. 6, *A, C,* and *E*, the nuclear membranes of apposed nuclei were closely associated but not fused. The distance between the nuclear membranes varied between 50–150 nm over as much as 1 μm of contact. Examination of both random and serial sections through nuclei demonstrated that they remained separated by two complete nuclear envelopes over the entire region of contact. All Class II mutants displayed this nuclear morphology, suggesting that there were no sub-categories for this mutant phenotype. This confirms that nuclear membrane fusion was not completed in all Class II mutant zygotes.

However, in some sections through apposed nuclei, membranous bridges were observed that spanned the gap between the two nuclei. Of 30 sections examined, 8 had 1 bridge and 2 had 2 bridges; we estimate that as many as 5 exist between nuclei. Bridges present in *kar2, kar5, kar7,* and *kar8* mutants were contained within a single section (Fig. 6, *G* and *H*). In

some favorable sections, the bridges appeared to be composed of two lipid bilayers (Fig. 6 *D* and data not shown). Some bridges found between *kar8* mutant nuclei appeared to contain a lumen and traversed several serial sections (Fig. 6 *I*). The exact nature and significance of these structures is uncertain. It is possible that the bridges are artifacts of EM preparation. However, because there are mutant specific differences and because they were only found between nuclei and not other membranous organelles, they might be real structures that arise from abortive attempts at nuclear membrane fusion.

By EM it is not possible to determine whether mixing of lumenal components can occur between the two nuclei. To test directly for membrane fusion defects and to determine whether lumenal mixing occurs, the new Class II mutations were assayed for homotypic ER membrane fusion in vitro (Latterich and Schekman, 1994). This assay is based on the intermixing of proteins in distinctly marked ER membranes. An acceptor membrane carries the wild-type Gls1p enzyme that trims terminal glucosyl residues from core glycosylated proteins in the ER (Esmon et al., 1984). The donor membrane carries a radioactively labeled substrate for Gls1p, glycosylated pro-α-factor (gpαF), in a *gls1-1* mutant background. The gpαF migrates at 32 kD in the *gls1-1* mutant membranes and is trimmed to 29 kD in wild-type *GLS1* membranes. Membrane fusion is measured by the percent trimming of the labeled gpαF to 29 kD during the reaction. In this assay, wild-type membrane fusion results in ~20% trimming; this activity is not stimulated by cytosol or mating factor and does not require the secretory proteins Sec17p (α SNAP) or Sec18p (NSF) (Latterich and Schekman, 1994). This suggests that nuclear membrane fusion is distinct from vesicle fusion in the secretory pathway.

When Class I mutants *kar1* and *kar3* were assayed by Latterich and Schekman (1994), they were not defective in this assay. As shown in Fig. 7, Class II mutants *kar5-486, kar5-1162,* and *kar8-1333* were dramatically reduced in activity relative to wild type at 30°C. Membrane fusion was defective regardless of whether donor, acceptor or both membranes were mutant, demonstrating that the mutants were unilateral in vitro. The *kar7* mutation displayed a temperature sensitive defect in vitro at 37°C that was similar to *kar2* mutants (Latterich and Schekman, 1994). The in vitro temperature sensitive defects suggest that the requirements for Kar2p and Kar7p are direct. Control experiments showed that the various *kar* mutant membranes were not defective in glucosidase activity or in membrane integrity; addition of Triton X-100 to reactions containing *kar* donor and acceptor membranes resulted in 90% trimming of gpαF (data not shown). We conclude that all Class II mutants display defects in vitro for mixing of ER/nuclear envelope lumenal contents which is in agreement with their in vivo defects for nuclear membrane fusion.

Discussion

In this paper we describe a novel bilateral mutant screen which uses a rapid mating type switch, a simple assay for ploidy, and microscopy to distinguish the different mutant classes. With this screen, we identified mutations in five new *KAR* genes and three new *FUS* genes which displayed strong bilateral defects. The *kar* mutants fell naturally into two dis-
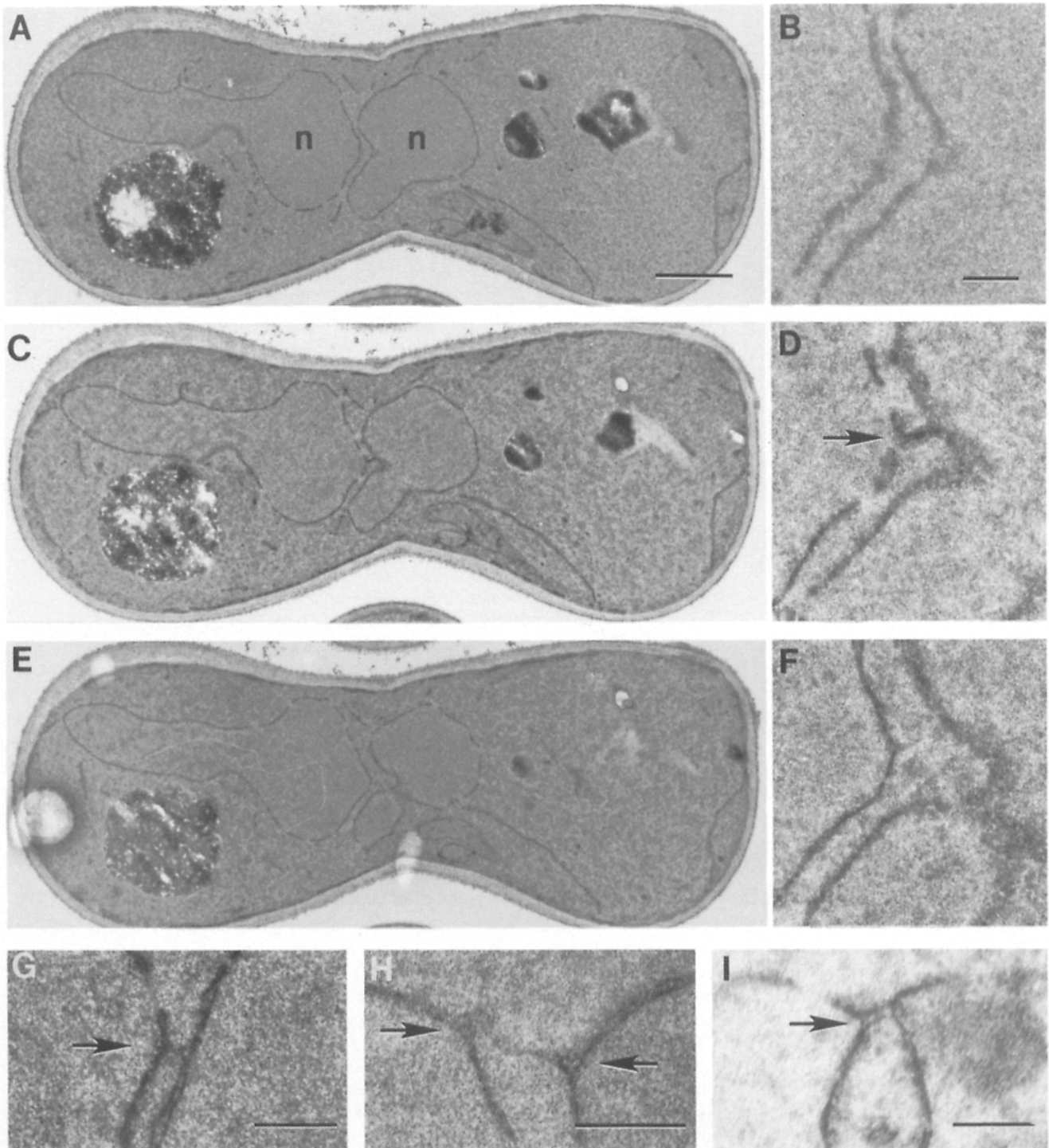
Figure 6. Class II zygotic nuclei make a direct contact but fail to fuse. (*A–F*) Electron micrographs of three consecutive serial sections (of ten) through a *kar5* mutant zygote (MS2689 × MS2690) are shown in two different magnifications. (*D, G,* and *H*) Representative bridges between *kar5* nuclei. (*I*) A morphologically distinct bridge between *kar8* nuclei (MS2705 × MS2706). Arrows denote bridges. Bars: (*A, C,* and *E*) 1 μm; (*B, D, F, G, H,* and *I*) 0.2 μm.

tinct classes based upon the distance between nuclei in mutant zygotes. The mutant classes represent at least two discrete stages in the functional pathway for karyogamy. Class I mutations block nuclear congression through microtubule defects. The cytoplasmic microtubules were abnormally long and failed to interconnect in *kar4* mutant zygotes. In *kar9* mutant zygotes, cytoplasmic microtubules were misoriented and failed to interconnect. The Class II mutants were defective for nuclear membrane fusion; nuclei in *kar2*, *kar5*, *kar7*, and *kar8* mutant zygotes were closely juxtaposed but failed to fuse. Putative membrane bridges were observed that may be the result of abortive nuclear fusion events. In
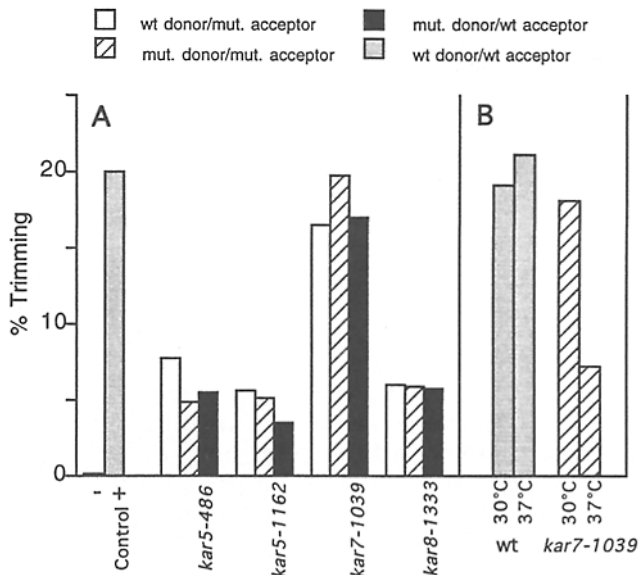
Figure 7. Class II mutations cause defects in vitro for ER/nuclear membrane fusion. Donor membranes (75 μg) and acceptor membranes (75 μg) derived from different *kar* mutants were incubated at the indicated temperature. Membranes were prepared as described in Latterich and Schekman (1994). At 30°C, *kar5-486* (MY3257, MY3258), *kar5-1162* (MY3259, MY3260), and *kar8-1333* (MY3256, MY3255) mutations caused defects in vitro for membrane fusion when present in donor, acceptor, or both membranes. *kar7* mutant membranes (MY3254, MY3253) were temperature sensitive in vitro for membrane fusion when cells were grown and membranes prepared at 30°C.
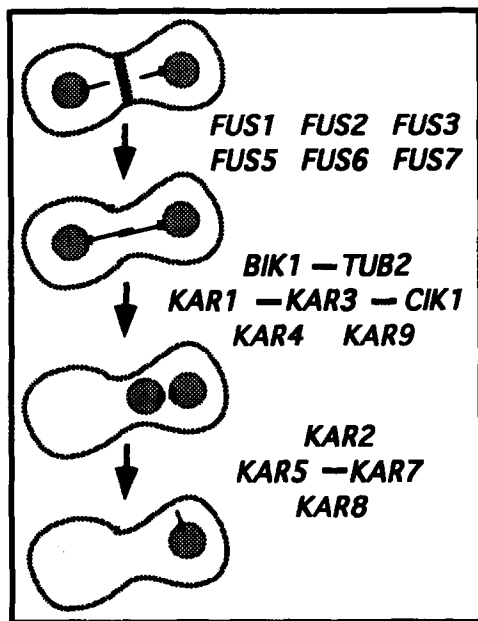
Figure 8. The pathway for karyogamy. *fus* mutants define the events which lead to cellular fusion during mating. Class I mutants define the first event in the karyogamy pathway, nuclear congression. These include genes required for SPB and cytoplasmic microtubule functions. Class II mutants define the second event in the karyogamy pathway, nuclear envelope fusion, which includes genes required for membrane fusion. Dashed lines between members indicate genetic interactions.

vitro, all Class II mutants were defective for homotypic ER/nuclear membrane fusion.

The Bilateral Screen

Although the screen allowed identification of both unilateral and bilateral mutations, nearly all mutations isolated were bilateral. The mutants may be bilateral because they are only required in one parent for efficient nuclear fusion. However, it is more likely that the *KAR* gene products are diffusible in vivo and are able to assemble and function after cell fusion. In the case of compartmentalized proteins such as membrane proteins required for nuclear envelope fusion, diffusibility may arise from new synthesis in the zygote. This view is suggested by the observation that bilateral mutations caused unilateral defects in vitro for membrane fusion. It seems likely that for most genes required for karyogamy, simple loss of function will generate a bilateral defect in vivo whereas unilateral phenotypes may be restricted to rather unusual alleles or genes.

The frequency of mutant isolation implies that the screen has not been saturated. Only one previously isolated gene was identified and most of the new genes identified had single alleles. From this outcome, we estimate that the target size for bilateral *KAR* and *FUS* genes is quite large. Since the screen detected general mating defects, many sterile mutants were also identified. Their frequency of isolation might be enhanced by their extreme mating defects which made them easier to identify; *kar* and *fus* mutations were more leaky and may have been discarded inadvertently during screening.

Only ten percent of mutants that failed to papillate displayed mutant phenotypes by microscopy; the remainder appeared to be wild type for zygote formation. It seems likely that the majority of these mutant candidates were wild-type colonies that, for stochastic reasons, had not appreciably recombined to generate a wild-type *HIS3* gene which is necessary for papillation. Multiple rounds of rescreening reduced the number of "wild-type" colonies, but at some frequency *kar* mutants will also form papillae. We therefore limited screening to discard a maximum of wild type without losing *kar* mutants. One possible class of mutations in this group may be those defective for adaption from pheromone-induced G1 arrest. These would efficiently form wild-type zygotes that would be unable to resume growth. Although they would appear wild type by microscopy, they would be bilateral sterile when assayed for diploid formation.

A Pathway for Karyogamy

Division of the *kar* mutants into classes defined two distinct steps during karyogamy. We believe the classes represent specific stages because the mutants fell into only two classes with little variation within a class or when different alleles of the same gene were assayed. Epistasis analysis revealed that, whatever the mechanism of the defects, steps required for nuclear congression precede steps leading to membrane fusion (Fig. 8).

Cytoplasmic microtubules appear to be required for nuclear congression and all Class I mutants displayed microtubule defects. *KAR1* and *KAR3* have both been shown to be essential for SPB and cytoplasmic microtubule functions during karyogamy. *KAR4* appears to play a regulatory role over two genes required for this process, *KAR3* and *CIK1*.

KAR9 may be required for spindle orientation and nuclear migration through interactions with microtubules or other proteins required for this process. It is also apparent that mutations in *TUB2*, *CIK1*, and *BIK1* will display a Class I phenotype based on their known functions involving microtubules.

Genes required for nuclear envelope fusion define the second event in the karyogamy pathway. As stated previously, the role of *KAR2* during karyogamy remained unclear. In this paper and that of Latterich and Schekman (1994), evidence is provided which suggests that *KAR2* plays a direct role in nuclear envelope fusion. The defect caused by the *kar7* mutation also appears to be direct since it is temperature sensitive in vitro. For *kar5* and *kar8* mutations, it was difficult to assess whether their defects were direct because conditional alleles were not available. However, since the addition of wild-type cytosol failed to complement the in vitro defects, all of these mutations appear to have caused specific nuclear membrane defects. The Class II Kar proteins may either be components of the nuclear envelope fusion apparatus or they may be required for the regulation or assembly of the fusion apparatus. From our analysis, it is not possible to resolve whether these proteins are required for early events such as membrane recognition or docking or the actual membrane fusion event.

It is interesting that the bilateral mutations displayed unilateral defects in vitro. It is possible that gene products which are bilateral because they are redundant in vivo may be limiting in vitro resulting in a unilateral defect. Also, in vivo, new synthesis of wild-type gene products occurs after cellular fusion and thus may complement a mutant nucleus. Although the mutants could not be complemented by wild-type cytosol in vitro, the cytosol was not obtained from pheromone-induced cells. It is possible that there are pheromone inducible components absent or in reduced quantities that are required for the proteins to become associated with the membranes for fusion.

Ostensibly, the morphology of Class II mutant nuclei differs from that described for wild-type nuclei undergoing fusion (Byers and Goetsch, 1974, 1975). Concomitant with cell fusion, wild-type nuclei became closely apposed only in the vicinity of the SPB and apparently fused at this site quickly thereafter. Due to the preparative techniques used, the exact disposition of the membranes during SPB fusion was not determined. In contrast, Class II mutant nuclei became apposed over a large region and remained this way after the completion of cell fusion. Although not visualized by our EM analysis, immunofluorescent microscopy showed that SPB fusion did not occur as indicated by two distinct vertices of tubulin staining in the region of apposition. In spite of these differences, we believe that the Class II mutant morphology reflects a temporal block in the normal process of nuclear fusion. From the data available, we expect that a single membrane fusion event occurs in the vicinity of the fusing SPBs. The putative bridges that were observed may be the result of abortive membrane fusion events which accumulate with time over the entire region of apposition. It is possible that a related precursor may form during wild-type nuclear fusion. If these structures represent attempts in fusion, they must not be productive because Class II mutants display defects in lumenal mixing when assayed in vitro. This predicts that Class II Kar proteins may be required for the

completion of membrane fusion. It will be very interesting to investigate how the two events of SPB and membrane fusion are coupled during karyogamy.

Because the in vitro assay is not stimulated by pheromone, the reaction is not likely to be mating specific. This therefore suggests that Class II proteins have functions that are required for vegetative growth, especially since two mutants display temperature sensitive growth defects. There are several processes during vegetative growth which may require homotypic fusion. One is in the dynamic biogenesis of the ER (Lee and Chen, 1988). Another is the recycling of ER resident components; vesicles containing ER derived proteins are returned from a post-ER compartment such that they are not lost to the forward flow of secretion (Semenza et al., 1990). Preliminary evidence indicates that some Class II mutants fail to retain ER resident proteins (Beh, C. T., and M. D. Rose, unpublished observation). Other possible defects in secretion and membrane physiology are currently under investigation, in particular, the phenotype of *kar5-1162* and *kar7-1039* at the non-permissive temperature.

It is possible that Class II *KAR* gene products will be related to those required in higher eukaryotes for the reformation of the nucleus after mitosis (Sullivan et al., 1993; Wiese and Wilson, 1993). A homologous yeast system would be an invaluable genetic tool for such studies. There may also exist homotypic fusion reactions that are specific to yeast. For example, although the nuclear envelope does not break down during mitosis, nuclear division does require membrane reorganization and intranuclear fusion to generate two nuclei. It is possible that components required for nuclear envelope fusion during karyogamy may also be required for nuclear envelope resolution during mitosis. These and other issues will be resolved by further characterization of the Class II *KAR* genes.

References

Berlin, V., J. A. Brill, J. Trueheart, J. D. Boeke, and G. R. Fink. 1991. Genetic screens and selections for cell and nuclear fusion mutants. *In* Guide to Yeast Genetics and Molecular Biology. C. Guthrie and G. R. Fink, editors. *Methods Enzymol.* 194:774–792.

Berlin, V., C. A. Styles, and G. R. Fink. 1990. *BIK1*, a protein required for microtubule function during mating and mitosis in *Saccharomyces cerevisiae*, colocalizes with tubulin. *J. Cell Biol.* 111:2573–2586.

Boeke, J. D., F. Lacroute, and G. R. Fink. 1984. A positive selection for mutants lacking orotidine 5'-phosphate decarboxylase activity in yeast: 5-fluoroorotic acid resistance. *Mol. Gen. Genet.* 181:288–291.

Byers, B. 1981. Cytology of the Yeast Life Cycle. *In* The Molecular Biology of the Yeast *Saccharomyces*: Life Cycle and Inheritance. J. N. Strathern, E. W. Jones, and J. R. Broach, editors. Cold-Spring Harbor, New York. 59–96.

Byers, B., and L. Goetsch. 1974. Duplication of spindle plaques and integration of the yeast cell cycle. *Cold Spring Harbor Symp. Quant. Biol.* 38:123–131.

Byers, B., and L. Goetsch. 1975. Behavior of spindles and spindle plaques in the cell cycle and conjugation in *Saccharomyces cerevisiae*. *J. Bacteriol.* 124:511–523.

Chan, C. S. M., and D. Botstein. 1993. Isolation and characterization of chromosome-gain and increase-in-ploidy mutants in yeast. *Genetics.* 135:677–691.

Conde, J., and G. R. Fink. 1976. A mutant of *Saccharomyces cerevisiae* defective for nuclear fusion. *Proc. Natl. Acad. Sci. USA.* 73:3651–3655.

Elion, E. A., P. L. Grisafi, and G. R. Fink. 1990. *FUS3* encodes a cdc2+/CDC28-related kinase required for the transition from mitosis into conjugation. *Cell.* 60:649–664.

Esmon, B., P. C. Esmon, and R. Schekman. 1984. Early steps in processing of yeast glycoproteins. *J. Biol. Chem.* 259:10322–10327.

Hoffman, C. S., and F. Winston. 1987. A ten minute DNA preparation from yeast efficiently releases autonomous plasmids for transformation of *E. coli. Gene (Amst.).* 57:267–272.

Huffaker, T. C., J. H. Thomas, and D. Botstein. 1988. Diverse effects of β-tubulin mutations of microtubule formation and function. *J. Cell Biol.* 106:1997–2010.

Ito, H., Y. Fukuda, K. Murata, and A. Kimura. 1983. Transformation of intact yeast cells treated with alkali cations. *J. Bacteriol.* 153:163–168.

Jacobs, C. W., A. E. M. Adams, P. J. Szaniszlo, and J. R. Pringle. 1988. Functions of microtubules in the *Saccharomyces cerevisiae* cell cycle. *J. Cell Biol.* 107:1409–1426.

Kaiser, C. A., and R. Schekman. 1990. Distinct sets of *SEC* genes govern transport vesicle formation and fusion early in the secretory pathway. *Cell.* 61:723–733.

Kassir, Y., and G. Simchen. 1976. Regulation of mating and meiosis in yeast by the mating-type region. *Genetics.* 82:187–206.

Koshland, D., and P. Hieter. 1987. Visual assay for chromosome ploidy. *In* Recombinant DNA, Part F; R. Wu, editor. *Methods Enzymol.* 155:351–372.

Latterich, M., and R. Schekman. 1994. The Karyogamy gene *KAR2* and novel proteins are required for ER membrane fusion. *Cell.* In press.

Lee, C., and L. B. Chen. 1988. Dynamic behavior of the endoplasmic reticulum in living cells. *Cell.* 54:37–46.

Mahoney, D. J., and J. R. Broach. 1989. The HML mating-type cassette of *Saccharomyces cerevisiae* is regulated by two separate but functionally equivalent silencers. *Mol. Cell. Biol.* 9:4621–4630.

McCaffrey, G., F. J. Clay, K. Kelsay, and G. F. Sprague. 1987. Identification and regulation of a gene required for cell fusion during mating of the yeast *Saccharomyces cerevisiae. MCB (Mol. Cell. Biol.)* 7:2680–2690.

Meluh, P. B., and M. D. Rose. 1990. *KAR3*, a kinesin-related gene required for yeast nuclear fusion. *Cell.* 60:1029–1041.

Page, B. D., and M. Snyder. 1992. *CIK1*: a developmentally regulated spindle pole body-associated protein important for microtubule functions in *Saccharomyces cerevisiae. Genes Dev.* 6:1414–1429.

Page, B. D., L. L. Satterwhite, M. D. Rose, and M. Snyder. 1994. Localization of the *KAR3* kinesin heavy chain-like protein requires the *CIK1* interacting protein. *J. Cell Biol.* 124:507–519.

Polaina, J., and J. Conde. 1982. Genes involved in the control of nuclear fusion during the sexual cycle of *Saccharomyces cerevisiae. Mol. Gen. Genet.* 186:253–258.

Rose, M. D. 1991. Nuclear fusion in yeast. *Annu. Rev. Microbiol.* 45:539–567.

Rose, M. D., and G. R. Fink. 1987. *KAR1*, a gene required for function of both intranuclear and extranuclear microtubules in yeast. *Cell.* 48:1047–1060.

Rose, M. D., L. M. Misra, and J. P. Vogel. 1989. KAR2, a karyogamy gene, is the yeast homolog of the mammalian *BiP/GRP78* gene. *Cell.* 57:1211–1221.

Rose, M. D., B. R. Price, and G. R. Fink. 1986. *Saccharomyces cerevisiae* nuclear fusion requires prior activation by alpha factor. *Mol. Cell. Biol.* 6:3490–3497.

Rose, M. D., F. Winston, and P. Hieter. 1990. Methods of Yeast Genetics. Cold Spring Harbor, New York. 198 pp.

Semenza, J. C., K. G. Hardwick, N. Dean, and H. R. B. Pelham. 1990. *ERS2*, a yeast gene required for the receptor-mediated retrieval of lumenal ER proteins from the secretory pathway. *Cell.* 61:1349–1357.

Sikorski, R., and P. Hieter. 1989. A system of shuttle vectors and yeast host strains designed for efficient manipulation of DNA in *Saccharomyces cerevisiae. Genetics.* 122:19–27.

Sullivan, K. M. C., W. B. Busa, and K. L. Wilson. 1993. Calcium mobilization is required for nuclear vesicle fusion in vitro: implications for membrane traffic and IP3 receptor function. *Cell.* 73:1411–1422.

Stearns, T., and D. Botstein. 1988. Unlinked noncomplementation: isolation of new conditional-lethal mutations in each of the tubulin genes of *Saccharomyces cerevisiae. Genetics.* 119:249–260.

Tachibana, C., and T. H. Stevens. 1992. The yeast *EUG1* gene encodes an endoplasmic reticulum protein that is functionally related to protein disulfide isomerase. *Mol. Cell. Biol.* 12:4601–4611.

Trueheart, J., J. D. Boeke, and G. R. Fink. 1987. Two genes required for cell fusion during yeast conjugation: evidence for a pheromone-induced surface protein. *Mol. Cell. Biol.* 7:2316–2328.

Vallen, E. A., M. A. Hiller, T. Y. Scherson, and M. D. Rose. 1992. Separate domains of *KAR1* mediate distinct functions in mitosis and nuclear fusion. *J. Cell Biol.* 117:1277–1287.

Wiese, C., and K. L. Wilson. 1993. Nuclear membrane dynamics. *Curr. Opin. Cell Biol.* 5:387–394.